miR-375-NAT10 Axis Dysfunction Promotes Oral Cancer Development and Mediates Cdk7 Stabilizing and Cell Cycle Progression

Chen ZOU
Foshan University
Xia LI
Foshan University
Haigang WEI
Foshan University
Siyuan WU
Foshan University
Jing SONG
Foshan University
Zhe TANG
Foshan University
Hailing LUO
Foshan University
Xiaozhi LV
Southern Medical University
Yilong Ai (aiyilong01@126.com)
Foshan University

Research

Keywords: oral cancer, NAT10, CDK7, cell cycle, Acetylation

Posted Date: July 29th, 2021

DOI: https://doi.org/10.21203/rs.3.rs-718593/v1

Abstract

Background: Oral cancer is the most common cancer with poor prognosis and outcome for the patients due to the challenging diagnosis and limited treatment possibilities. However, the molecular underpinnings behind the malignant progression of oral cancer remain incompletely understood.

Methods: The expression profiling of NAT10 and CDK7 in oral cancer patients were assessed by IHC, qPCR and western blots. ShRNA was used to silence gene expression. The biological function of NAT10 and CDK7 in cholangiocarcinoma was investigated using in vitro and in vivo studies including, transwell cell migration, plate cloning, CCK8, shRNA interference, western blots, flow cytometry and xenograft mouse model. The underlying molecular mechanism was determined by western blots and immunoprecipitation.

Results: In this study, we demonstrated that deregulation of miR-375-NAT10 axis is among the most causes in inducing the acquisition of a tumorigenesis phenotype in oral cancer cells. NAT10 is abundant in oral cancer tissue. and its protein level is positively correlated with poor overall survival. Increased the level of NAT10 promotes oral cancer cell proliferation in vitro as well as xenograft tumorigenicity in vivo. Most importantly, NAT10 regulates cancer cell proliferation through stabilizing CDK7 thus regulating the cell cycle. NAT10 as an acetyltransferase is responsible for CDK7 acetylation at lysine 328 (K328Ac). Moreover, it was found that the expression of miR-375 is abnormally alleviated in oral cancer tissues. Bioinformatics analysis revealed a targeted complementary binding site between miR-375 and NAT10. Decreased expression of miR-375 promotes expression of NAT10.

Conclusion: Our study showed that NAT10 plays a strong carcinogenic role in oral cancer tumorigenesis by acetylating CDK7 at K382 thus promotion stability. Moreover, NAT10 may serve as a target for miR-375. Therefore, targeting NAT10 may provide a new and effective therapeutic strategy to inhibit the tumorigenicity of oral cancer.

Background

Oral cancer is the eighth most common cancer, with an estimated 657,000 new cases and 330,000 deaths annually in 2020, and these numbers are expected to double by 2035 according to the World Health Organization (WHO)[1–3]. Squamous cell carcinomas (OSCCs) account for 90%[4,5]. Early oral cancer usually presents as subtle mucosal lesions classified as oral potentially malignant disorders (OPMD) [6,7]. Early oral cancers are frequently asymptomatic and occult[8,9]. Therefore, the majority of OSCCs are diagnosed at the advanced stages, the prognosis of patients with OSCC is poor with a 5-year survival rate less than 30% [10,11]. Early detection and effective treatment of these lesions are essential to improve the survival rate and prevent the progression of oral cancer. Although surgical resection, radiotherapy, chemotherapy and other comprehensive treatment methods have been widely used in the treatment of oral cancer, the treatment effect remains not satisfactory[12,13]. The patient's prognosis is poor and the survival rate is low.

N-acetyltransferase 10 (NAT10) is a member of the GNAT family of KATs and has been documented to acetylate RNA[14–16], NAT10 or a homologous enzyme in other species increased the formation of ac4C on tRNA, rRNA, and mRNA, thereby maintaining the accuracy of protein translation and stabilizing the mRNA[15,17]. Transcriptional cofactor Che-1, hTERT and T-tubulin were also documented as substrates of NAT10[14,18–20]. Moreover, deregulation of NAT10 has been implicated in Hutchinson Gilford progeria syndrome[15,21,22]. NAT10 was associated with cancer by demonstrating that it could significantly promote cell growth in epithelial ovarian cancer and breast cancer[23,24]. NAT10 also has a potential role in increasing melanogenesis and melanoma growth[25,26]. However, NAT10 inhibits cell proliferation and expression of NAT10 decreases in human colorectal carcinomas[14]. These findings suggest that NAT10 has multifaceted functional roles in cancers. However, the underlying functions and mechanisms of NAT10 in oral cancer progression remain unknown.

Among the CDKs regulating DNA transcription, CDK7 is the most critical one. It activates mRNA synthesis by phosphorylating the carboxyl terminal domain (CTD) of the largest subunit of RNA polymerase II (RNAPII)[27,28]. CDK7 and its partners, cyclin H and MAT1, were originally isolated as a CDK-activating kinase (CAK), which is necessary for the complete activation of CDKs in cell cycle[29,30]. CDK7 deficient mouse model deficiency showed early embryonic lethality[31], which indicates its importance in development. Recently, CDK7 has been increasingly recognized for its role in breast cancer, T cell acute lymphoblastic leukemia, gastric cancer, small cell lung cancer, neuroblastoma and ovarian cancer[32–36]. As an anticancer target, the inhibition of CDK7 with small molecules THZ1 has been considered to be a promising cancer therapy[37,38]. There are several ongoing preclinical studies and clinical trials to examine CDK7 inhibitors in advanced solid malignancies.

Materials And Methods

Patients

This study was approved by the Ethical Committee of Foshan Stomatological Hospital. All patients signed an informed-consent document for diagnosis and research on tissue specimens before being enrolled in the project.

Animals

All the animal experiments were approved by Animal Care and Use Committee of Foshan University. Then, extensive efforts were made to minimize the pain of the animals used in the study.

In vivo tumor growth assay

A total of 12 male athymic Balb/c nude mice (aged 6 weeks old and weighing 20 ~ 23 g) were injected with about 1 × 107 OECM1 cells resuspended with 200 μL PBS. Mice were treated with a remodelin dose of 100 mg per kg orally after injection, until the end-point. Tumor volumes was measured every 3 to 4 days (2 times a week). When the tumor grew into a certain size, the tumor size was calculated with the

following formula:(π × length × width2)/6. After the mice were euthanized, the tumor size and weight were measured.

Cell lines and cell culture

The HOK, HSC3, OECM1, KG005, SCC4 and SCC25 cell lines were purchased from the Cell Resource Center of the Shanghai Institute of Life Sciences, Chinese Academy of Sciences and authenticated by short-tandem repeat testing. Each cell line was mycoplasma-free and cultured in RPMI-1640 medium (Gibco; Thermo Fisher Scientific, Inc.) containing 10% fetal bovine serum (Gibco; Thermo Fisher Scientific, Inc.) and 1% penicillin-streptomycin (Gibco; Thermo Fisher Scientific, Inc.) in an incubator at 37 ˚C with 5% CO_2.

Construction of lentivirus and stable transfection into cell lines

The lentiviral vector encoding the human NAT10 gene was constructed by Genechem Co., Ltd. Lentiviral vector coding shRNA targeting NAT10 and shRNA negative control were designated as shNAT10 and shNC, respectively. The target sequences were as follows: shNAT10 #1, 5'- AUGGAACACUGAACAUAAATT-3'; and shNAT10 #2, 5'- GGCCAAAGCUGUCUUGAAATT – 3'. The cells were transfected with recombinant lentivirus-transducing units in the presence of polybrene (6 μg/ml) according to the manufacturer's instructions and stable NAT10 knockdown clones were selected by 2.5 μg/ml puromycin (A1113803; Gibco; Thermo Fisher Scientific, Inc.). The selected pools of knockdown cells were then collected and cultured within 10 passages for use for subsequent experiments. Tables S2 and S3 provide detailed information on the expression structure and primers used for molecular cloning.

Co-Immunoprecipitation Assay and Immunoblotting

For immunoblotting analysis, modified RIPA lysis buffer (50 mM Tris-HCl, pH = 7.4, 1% Nonidet P-40, 0.25% sodium deoxycholate, 150 mM NaCl, and 1 mM EDTA) with supplements of protease inhibitors as well as phosphatase inhibitors (Bimake, Houston, USA) were used to lyse cells. The BCA protein assay reagent (Yeasen, Shanghai, China) was used to examinate protein concentrations. Cell extracts were first decomposed by SDS-PAGE and then applied to PVDF membrane (Billerica millipore, USA). Then, they were incubated by the appropriate primary antibodies. Later, enhanced chemiluminescent substrate kit (Yeasen) was utilized to analyze the specific signals of indicated antibody. For immunoprecipitaton of endogenous proteins, primary antibodies or control IgG were used to incubate cell extracts in a rotating incubator overnight at temperature of 4°C, then the products were incubated for another 3 h with protein A/G magnetic beads (Sigma-Aldrich, St. Louis, MO, USA). The beads were washed three times using lysis buffer before immunoblotting analysis.

Reverse transcription quantitative polymerase chain reaction (RT-qPCR)

Total RNA was extracted by TRIzol reagent (Invitrogen; Thermo Fisher Scientific, Inc.) and reverse transcribed using the ThermoScript RT-PCR system (cat. no. 11731015; Invitrogen; Thermo Fisher Scientific, Inc.) according to the manufacturer's protocol. qPCR with SYBR-Green (cat. no. 1708886; Bio-Rad Laboratories, Inc.) were performed on an iQ5 Multicolor Real-Time PCR Detection system (Bio-Rad Laboratories, Inc.). The PCR conditions were as follows: 95 ˚C for 5 min followed by 40 cycles of 95 ˚C for 30 s and 57 ˚C for 30 s. GAPDH was used as an internal control. All reactions were run in triplicate and quantified with 2-ΔΔCq[62].

Western blot analysis

The cells were collected and lysed with immunoprecipitation assay buffer (NP40 buffer) added with protease inhibitor cocktail (Roche Applied Science). Lysates were fractionated by 10% SDS-PAGE and subsequently transferred onto nitrocellulose membranes (Hybond C; GE Healthcare Life Sciences). The membranes were blocked with 5% non-fat milk for obstructed non-specific binding sites at room temperature for 1 h and then incubated with the following antibodies overnight at 4˚C: Anti-NAT10 (ab194297; dilution, 1:1000; Abcam), CDK7 (ab256787; dilution, 1:1000; Abcam), Vinculin (ab219649; dilution, 1:1,000, Abcam), CDK1 (ab133327; dilution, 1:1,000, Abcam), CDK2 (ab32147; dilution, 1:1,000, Abcam) Phospho-CDK1 (ab201008; dilution, 1:1,000, Abcam), Phospho-CDK2 (#2561; dilution, 1:1,000, Cell Signaling Technology). Membranes were then washed three times and then incubated with HRP-conjugated goat anti-rabbit (#7074; dilution, 1:500) or goat anti-mouse (#7076; dilution, 1:500) antibodies (both from Cell Signaling Technology). The bands were visualized by enhanced chemiluminescence reagents (cat. no. WP20005; Thermo Fisher Scientific, Inc.).

Cell proliferation assay

Cell proliferation was measured by cell count methods. For CCK-8 assay (Keygen Biotech), the cells were inoculated in 96-well plates in triplicate and observed every day, 10 μl CCK-8 and 100 μl fresh medium were added to each well and at specific time-points and then incubated for 3 h at 37 ˚C, the absorbance was measured at 450 nm using a microplate reader (ST-360; KHB). For colony-formation assay, stable cells were inoculated in six-well plates in triplicate and cultured for 14–21 days. The cells were then fixed with 4% paraformaldehyde and stained with crystal violet staining solution. Visualize colonies were counted.

Flow cytometric evaluation

The cells were then collected and washed with cold PBS. Annexin V-FITC reagent kit (cat. no. A211-01; Vazyme Biotech Co., Ltd.) was used to perform analysis. The cells were re-suspended in annexin V binding buffer with the final concentration of $1x10^6$ cells/ml and incubated with AnnexinV-FITC for 15 min at 4 ˚C in the presence of propidium iodide. Samples were analyzed using a BD FACSCalibur flow cytometer (BD Biosciences) and then analyzed were performed with FlowJo software (FlowJo 10.5, LLC).

Dual-luciferase reporter gene assay

The genomic DNA was extracted from OECMs. Then the NAT10 3'UTR sequence containing the putative binding site for miR-375 was amplified. GeneArt™ site-directed Mutagenesis PLUS System (ThermoFisher, Waltham, MA, USA) was used to mutate the sequences. The target sequences were collected after gel electrophoresis of the amplified products, and then inserted into the pmirGLO dualLuciferase miRNA Target expression vector (Promega, Madison, WI, USA) to construct the reporter vectors: NAT10 wild type (WT) and NAT10 mutant (MUT). After the sequence of the reporter vectors were sequenced by Sangon Biotech (Shanghai, China) with sequencing, the reporter vectors were transfected into the cells respectively, together with miR-375 mimics or NC mimics. The medium was discarded after 48 h. The cells were washed with PBS and then lysed with cell lysis buffer. After centrifugation at 3000×g for 5 min, the supernatant was collected and the luciferase activity was detected by dual luciferase reporter assay system (Promega, Madison, WI, USA).

Statistical analysis

All experiments were performed at least 3 independent experiments independently, and all values were expressed as the means ± standard deviation. The SPSS 20.0 software (IBM Corp.) was used for statistical analysis. A two-tailed unpaired Student's t-test with Welch correction or one-way ANOVA followed by Dunnett's adjustment (for dose-response effects) or the Bonferroni test (for multiple comparisons) was used to determine the statistical significance of the differences in the measured variables. A value of $p < 0.05$ was considered to indicate a statistically significant difference.

Results

Increased mRNA and protein level of NAT10 in oral cancer tissues

In order to identify the regulatory molecules that play a major role in the progression of oral cancer, we searched the public database (http://tumorsurvival.org) and found that patients with high expression of NAT10 had significantly poor prognosis in HNSCC patients (Fig. 1A and Supplementary Figure S1A). Subsequently, immunohistochemical staining was performed in 80 samples from oral cancer patients who underwent surgical resection in the Foshan Stomatological Hospital. The results also confirmed the negative regulatory effect of NAT10 on the prognosis of oral cancer patients (Fig. 1B-1C). The expression of NAT10 genes was investigated in oral tumor mRNA expression profiles. Analysis of publicly available microarray data revealed a highly significant upregulation of NAT10 mRNA in oral tumors compared to normal oral tissues (Fig. 1D). In order to confirm the expression of NAT10 in oral cancer, RT-PCR was performed in oral tumor containing 21 normal and 54 tumor samples. Results confirmed the elevated expression of NAT10 with significant fold change in all oral tumor tissue (Fig. 1E). We also observed that the expression of NAT10 increased with the progression of tumor stage in the public database (Fig. 1F). We confirmed the elevated expression of NAT10 with the progression of tumor staging using RT-PCR in 54 oral tumor samples (Fig. 1G).

NAT10 promotes the proliferation of oral cancer cells

We investigated the expression level of NAT10 in oral cancer cell lines. We observed that the expression of NAT10 in OECM1 and KG005 was in the middle level among those cell lines (Supplementary Fig. S1B), we selected OECM1and KG005 for the next proliferation experiments. we overexpressed NAT10 in OECM1 and KG005 cells (Fig. 2A-2B), and considerable promotions of growth in CCK8 and plate cloning assays were observed in both OECM1 and KG005 cells with the overexpression of NAT10 (Fig. 2C-2G). We treated OECM1 and KG005 cells with NAT10 enzymatic inhibitor, remodelin. We observed that the addition of remodelin significantly inhibited proliferation of OECM1 and KG005 cells in CCK8 and plate cloning assays (Fig. 2H-2L). Furthermore, we designed two NAT10 shRNAs to down-regulated NAT10 in OECM1and KG005 cells. As shown in Fig. 2M-2N, the protein level of NAT10 significantly reduced in OECM1and KG005 cells after NAT10 knockdown (Fig. 2M-2N). And the NAT10 knockdown obviously inhibited the proliferation of OECM1 and KG005 cells in CCK8 and plate cloning assays (Fig. 2O-2S). Thus, these results suggested that NAT10 promotes the proliferation of oral cancer cells in vitro.

NAT10 advances the tumorigenesis of oral cancer by upregulating CDK7 expression to promote the cell cycle

To further characterize the regulatory effect of NAT10 on cell proliferation. We next investigated the effect of NAT10 on cell cycle. As shown in Fig. 3A-3B, the population of cells arrested at G2/M phase was significantly increased in NAT10-knockdown OECM1 cells (Fig. 3A-3B). In addition, the number of cells arrested at G2/M phase was high in remodelin-treated OECM1 cells (Fig. 3C-3D). To elucidate how NAT10 suppression delays cell cycle progression, an integrated bioinformatics platform (BioGRID) for investigating the protein interaction network (https://thebiogrid.org) was utilized to predict the partners of NAT10. We performed GO analysis to the molecules predicted by the website that interact with NAT10, we observed that these molecules are enriched in rRNA processing, DNA repair, cell cycle and so on (Fig. 3E). Considering the effect of NAT10 on cell cycle, we noticed that CDK7 may serve as a binding partner for NAT10 (Fig. 3E). CDK7 has essential role in both the cell-division cycle and transcription. To achieve this, we next examined whether CDK7 interacts with NAT10. The interaction between CDK7 and NAT10 at the endogenous protein levels was validated in OECM1 and KG005 cells by co-immunoprecipitation with an anti-CDK7 antibody and anti-NAT10 (Fig. 3F). Then we explored the interaction between CDK7 and NAT10 at the exogenous protein levels in HEK293T cells. We also obtained a similar result at the exogenous protein levels (Fig. 3G). By silencing NAT10, we discovered that the protein level of CDK7 was significantly decreased in OECM1 and KG005 cells (Fig. 3H-3I). Overexpression of NAT10 increase the level of CDK7 in OECM1 and KG005 cells (Fig. 3J-3K). The treatment of remodelin have a negative regulation on expression of CDK7 in OECM1 and KG005 cells (Fig. 3L-3M). These findings might indicate NAT10 promotes the protein level of CDK7. Meanwhile, the positive correlation between NAT10 and CDK7 was observed in 6 clinical sample (Fig. 3N). Therefore, these results provided the important clues that NAT10 may promote the tumorigenesis of oral cancer via upregulating CDK7 level.

NAT10 upregulates CDK7 expression on protein level

We next further study whether the regulation of NAT10 on CDK7 is at the RNA level or protein level. The results demonstrated that NAT10 depletion by two respective shRNAs did not affect mRNA levels of

CDK7 but significantly reduced its protein levels in OECM1 and KG005 cells, and the increased NAT10 also have no influence in mRNA levels of CDK7 (Fig. 4A-4D). Furthermore, addition of MG132 with OECM1 and KG005 cells rescued decreased CDK7 induced by knockdown of NAT10 (Fig. 4E-4F). Those results suggested NAT10 play a regulatory role for CDK7 on protein level. As shown in Fig. 4G, H, the half-life of CDK7 in OECM1 cells expressing shNAT10 #1 and shNAT10 #2 was remarkable shorter than that in cells expressing shNC, indicating that NAT10 enhances the stability of CDK7 protein (Fig. 4G-4H). The treatment of remodelin also decrease half-life of CDK7 in OECM1 cells (Supplementary Figure S2A-S2B). In agreement with these observations, OECM1 cells were transfected with pCDH and NAT10. After 48 hours of transfection, cells were treated with 10 μM MG-132 for 6 hours and then total cellular lysates were subjected to IP assays with anti-CDK7 antibody. Immunoblotting analysis showed that NAT10 knockdown significantly decreased the ubiquitination of CDK7 protein (Fig. 4I).

CDK7 is acetylated at lysine 328 by NAT10

As NAT10 is a novel KAT with intrinsic acetyltransferase activities (41–46), we next investigated whether NAT10 acetylates CDK7. Results showed that ectopic expression of wildtype NAT10 but not its catalytically inactive mutant (G641E) enhanced acetylation of CDK7 in OECM1 and KG005 cells (Fig. 5A-5B). Conversely, knockdown of NAT10 using two independent shRNAs reduced acetylation of CDK7 (Fig. 5C-5D). In support of these findings, inhibition of NAT10 activity using the small molecule inhibitor remodelin also decreased acetylation of CDK7 (Fig. 5E). For further verification, we predicted the acetylation site lysine 382 of CDK7 through the PLMD website (http://plmd.biocuckoo.org) and mutated lysine 382 to arginine. The results showed that the mutation of lysine 382 significantly weaken the acetylation of CDK7 (Fig. 5F), which indicated that lysine 382 is the major acetylated site of CDK7. NAT10 play a regulatory role on acetylation and stability of CDK7. Glutamine (Q) is a mimic of acetylation mutation. To achieve the effect of K382 mutation on stability of CDK7, we treated OECM1 cells with CHX. the half-life of CDK7 in OECM1 cells expressing K328Q was remarkable longer than that in cells expressing wildtype (Fig. 5G), indicating that acetylation enhances the stability of CDK7 protein.

NAT10 promotes tumorigenesis of oral cancer through regulating CDK7

We also elaborate relative expression of NAT10 and CDK7 in clinical sample. The positive correlation between NAT10 and CDK7 was confirmed in those clinical sample (Fig. 6A-6B). The results demonstrated that engraft tumors in mice treated with remodelin grew lower than those treated DMSO, but CDK7 re-overexpression partly restored growth rate of engraft tumors (Fig. 6C-6E). CDK7 re-overexpression restored growth rate of remodelin treated OECM1 cells in vitro (Fig. 6F-6H). CDK7 re-overexpression also restored proliferation of OECM1 cells expressed shNAT10 (and supplementary FigureS3A-S3C). The treatment of remodelin arrested OECM1 cells in G2/M phase, but CDK7 re-overexpression impaired the arrest (Fig. 6I-6J). CDK7 is necessary for the complete activation of CDKs in cell cycle. We examined phosphorylation of CDK1 and CDK2, results suggested addition of remodelin and NAT10 knockdown significant reduced phosphorylation of CDK1 and CDK2 but re-overexpression of CDK7 in NAT10

knockdown cells restore the phosphorylation (Fig. 6K-6L). Those results demonstrated that NAT10 promotes cell cycle and tumorigenesis of oral cancer through regulating CDK7.

miR-375 targeted and regulated NAT10 in oral cancer

microRNAs (miRNAs) have been demonstrated to participate in the pathological process of oral cancer. We tended to investigate the upstream microRNAs of NAT10, which also play a major role in oral cancer. we determine upstream microRNA of NAT10 analysis based on the public miRNA predicted website (http://www.targetscan.org). We observed that NAT10 was one of the potential targets of miR-375 (Fig. 7A). Thus, dual-luciferase reporter gene assay was performed, and it was observed that miR-375 mimics remarkably reduced the luciferase activity of NAT10 WT reporter but not NAT10 MUT (Fig. 7B). Consistently, miR-375 inhibitor increased the luciferase activity of NAT10 WT reporter but not NAT10 MUT (Supplementary Figure S4A). We further determined the expressions of NAT10 using qRT-PCR and Western blot. It was found that the over-expression of miR-375 inhibited but inhibition of miR-375 increase the expression levels of NAT10 at both mRNA and protein levels (Fig. 7C-7E and Supplementary Figure S4B-S4D). We also verified the negative correlation between NAT10 and miR-375 in clinical sample (Fig. 7F). Collectively, it was confirmed that NAT10 serve as a target of mi-375 in oral cancer. Subsequently, we observed the expression of miR-37 in oral cancer is remarkably upregulated than normal tissue in predicted website also in our clinical sample (Fig. 7G-7I). Those results confirmed that miR-375 serve as upstream of NAT10 and CDK7 in oral cancer.

Discussion

Oral squamous cell carcinoma arises from the oral cavity, which includes hard and soft plate, tongue, floor of mouth, buccal mucosa and alveolar rim, oropharynx, hypopharynx and larynx of head and neck[39,40]. It is one of the six most common cancers in the world. Annually, approximately 45,780 new cases of OSCC in the United States, 61,400 in Europe, and 274,000 in Asia[41–43]. The OSCC is the leading cause of cancer deaths in the East Asian countries[44].

Important risk factors in the development of the disease are tobacco, betel quid, alcohol, age, gender and sunlight, although a role for candida and the human papilloma virus has also been documented[45,46]. The increase in alcohol consumption is associated with an increased incidence rate of OSCCs as tobacco consumption decreases[43,47]. When tobacco and alcohol are taken together, the carcinogenic action of tobacco and alcohol is synergistic[43,47]. The risk of oral cancer of alcoholics and smokers is 38 times higher than that of abstainers[48]. In addition, considering the amount of alcohol consumed by binge drinking, it is considered to be of particular importance in the malignant development of young people[49,50]. Historically, the risk of oral cancer increased with age[51,52]. Many patients however do not have history of any those habits and/or evidence of previous viral infection[53]. Therefore, additional factors are likely to cause OSCC in this subgroup. Genetic aberrations and predispositions are likely to be important and previous studies have identified a number of oncogenes and tumor suppressor genes that are involved in the pathogenesis of OSCC[54–56]. Better understanding of these genetic factors and

molecular mechanisms underlying the oral carcinogenesis and metastasis is important to improve the diagnosis, therapeutic options, prognosis and prevention of OSCCs.

Recently, microRNAs (miRNAs) have been documented potentially culminate in the development and progression of oral cancer. Different from deregulation of mRNA expression levels, miRNA expression alterations are mostly due to promoter-related changes[1,57,58]. The role of miRNA deregulation in oral cancer have been explored in several studies, therein, presenting compelling evidence for the involvement of miRNAs in angiogenesis, tumor progression, invasion, etc[58–60]. However, the regulatory mechanisms behind miRNA expression deregulation at a genome scale remained largely unknown.

NAT10 has been reported to promote formation of ac4C on tRNA, rRNA, and mRNA and protein acetylation[14,17]. Limited literature reported that its dysfunction plays an important role in some tumors[61], and its regulatory role in oral cancer remains unknow. Here we demonstrated a new acetylated substrate CDK7 for NAT10, and confirmed the regulatory role of NAT10 in cell cycle. NAT10 enzymatic inhibitor, remodelin, significantly inhibit the proliferation of oral cancer cells in vitro and in vivo, which provides a research foundation for the targeted therapy of NAT10 in oral cancer.

In this article, we also investigated the role of small RNA mediated regulation of oncogene in oral cancer. We have extensively described the role of miR-375 in regulating carcinogenesis in OSCC. We also discussed the role of miRNA mediated transcriptional repression of NAT10 in oral cancer. A comprehensive understanding of the miRNA regulation of oncogene in oral cancer may help to develop better strategies for the diagnosis, molecular targeted therapy and overall prognosis of oral cancer.

Conclusion

Our results unveil NAT10 as a potential diagnostic, prognostic and therapeutic tool for oral cancer, which provides a novel approach for use in noninvasive screening of oral cancer. Findings presented here show that NAT10 plays a progressive role in oral cancer progression (Fig. 8). NAT10 exerts its tumorigenic progressive functions through acetylated-dependent of CDK7. NAT10 functions as a tumor promoter to participate in cell cycle of oral cancer. Deregulated miR-375 increased the transcriptional level of NAT10. Consequently, evaluating the therapeutic potential of NAT10 in oral cancer deserve large-scale studies.

Abbreviations

shNC: shRNA negative control; shNAT10: shRNA targeting NAT10; OSCC: Oral squamous cell carcinoma; HNSCC: Squamous cell carcinoma of head and neck; OS: overall survival; RT-qPCR: reverse transcription quantitative polymerase chain reaction.

Declarations

Ethics approval and consent to participate

All experiments were performed in accordance with the Guidelines of the Care and Use of Laboratory Animals Monitoring Committee of Foshan Stomatological Hospital, School of Medicine, and Experiments were approved by the ethics committee at Foshan Stomatological Hospital, School of Medicine. Informed consents were obtained from human participants of this study.

Consent for publication

Not applicable.

Availability of data and material

The datasets generated and/or analyzed in this study are available from the respective author upon reasonable request.

Competing interests

The authors declare that there is no conflict of interest regarding the publication of this paper.

Funding

This research is supported by the science and technology cooperation between the government and the research and development project of Guangdong Natural Science Foundation.

Authors' contributions

ZC, AYL and LX conceived-designed experiment and wrote the manuscript. WHG, LXZ and WSY performed experiments. SJ, TZ and LHL analyzed data and prepared the figures. All authors reviewed the manuscript.

Acknowledgements

We would like to express our great appreciation to our colleagues for their valuable and constructive suggestions as well as technical support for this research work.

References

1. Hema KN, Smitha T, Sheethal HS, Mirnalini SA. Epigenetics in oral squamous cell carcinoma. Journal of oral maxillofacial pathology: JOMFP. 2017;21:252–9. doi:10.4103/jomfp.JOMFP_150_17.
2. Hawkins AT, et al. Diverticulitis: An Update From the Age Old Paradigm. Curr Probl Surg. 2020;57:100862. doi:10.1016/j.cpsurg.2020.100862.
3. Singhavi HR, et al. Comparison of the seventh and eighth editions American Joint Committee Cancer classification system in oral cavity squamous cell cancers. International journal of cancer. 2020;146:3379–84. doi:10.1002/ijc.32720.

4. Smyth EC, et al. Oesophageal cancer. Nature reviews Disease primers. 2017;3:17048. doi:10.1038/nrdp.2017.48.
5. Abnet CC, Arnold M, Wei WQ. Epidemiology of Esophageal Squamous Cell Carcinoma. Gastroenterology. 2018;154:360–73. doi:10.1053/j.gastro.2017.08.023.
6. Huang SH, O'Sullivan B. Oral cancer: Current role of radiotherapy and chemotherapy. *Medicina oral, patologia oral y cirugia bucal* **18**, e233-240, doi:10.4317/medoral.18772 (2013).
7. Gigliotti J, Madathil S, Makhoul N. Delays in oral cavity cancer. Int J Oral Maxillofac Surg. 2019;48:1131–7. doi:10.1016/j.ijom.2019.02.015.
8. Femiano F, et al. Oral malignant melanoma: a review of the literature. Journal of oral pathology medicine: official publication of the International Association of Oral Pathologists the American Academy of Oral Pathology. 2008;37:383–8. doi:10.1111/j.1600-0714.2008.00660.x.
9. Yan K, Agrawal N, Gooi Z. Head and Neck Masses. Med Clin N Am. 2018;102:1013–25. doi:10.1016/j.mcna.2018.06.012.
10. Wuerdemann N, et al. Risk Factors for Overall Survival Outcome in Surgically Treated Human Papillomavirus-Negative and Positive Patients with Oropharyngeal Cancer. Oncology research treatment. 2017;40:320–7. doi:10.1159/000477097.
11. Nemes JA, Redl P, Boda R, Kiss C, Márton IJ. Oral cancer report from Northeastern Hungary. Pathology oncology research: POR. 2008;14:85–92. doi:10.1007/s12253-008-9021-4.
12. Soukas AA, Hao H, Wu L. Metformin as Anti-Aging Therapy: Is It for Everyone? Trends Endocrinol Metab. 2019;30:745–55. doi:10.1016/j.tem.2019.07.015.
13. Eldredge JB, Spyropoulos AC. Direct oral anticoagulants in the treatment of pulmonary embolism. Curr Med Res Opin. 2018;34:131–40. doi:10.1080/03007995.2017.1364227.
14. Liu X, et al. NAT10 regulates p53 activation through acetylating p53 at K120 and ubiquitinating Mdm2. EMBO Rep. 2016;17:349–66. doi:10.15252/embr.201540505.
15. Larrieu D, Britton S, Demir M, Rodriguez R, Jackson SP. Chemical inhibition of NAT10 corrects defects of laminopathic cells. Science. 2014;344:527–32. doi:10.1126/science.1252651.
16. Liu HY, et al. Acetylation of MORC2 by NAT10 regulates cell-cycle checkpoint control and resistance to DNA-damaging chemotherapy and radiotherapy in breast cancer. Nucleic acids research. 2020;48:3638–56. doi:10.1093/nar/gkaa130.
17. Dominissini D, Rechavi G. N(4)-acetylation of Cytidine in mRNA by NAT10 Regulates Stability and Translation. Cell. 2018;175:1725–7. doi:10.1016/j.cell.2018.11.037.
18. Chi YH, Haller K, Peloponese JM Jr, Jeang KT. Histone acetyltransferase hALP and nuclear membrane protein hsSUN1 function in de-condensation of mitotic chromosomes. J Biol Chem. 2007;282:27447–58. doi:10.1074/jbc.M703098200.
19. Fu D, Collins K. Purification of human telomerase complexes identifies factors involved in telomerase biogenesis and telomere length regulation. Molecular cell. 2007;28:773–85. doi:10.1016/j.molcel.2007.09.023.

20. Liu X, et al. Deacetylation of NAT10 by Sirt1 promotes the transition from rRNA biogenesis to autophagy upon energy stress. Nucleic acids research. 2018;46:9601–16. doi:10.1093/nar/gky777.
21. Balmus G, et al. Targeting of NAT10 enhances healthspan in a mouse model of human accelerated aging syndrome. Nature communications. 2018;9:1700. doi:10.1038/s41467-018-03770-3.
22. Larrieu D, et al. Inhibition of the acetyltransferase NAT10 normalizes progeric and aging cells by rebalancing the Transportin-1 nuclear import pathway. Sci Signal 11, doi:10.1126/scisignal.aar5401 (2018).
23. Zhang X, et al. Cytosolic THUMPD1 promotes breast cancer cells invasion and metastasis via the AKT-GSK3-Snail pathway. Oncotarget. 2017;8:13357–66. doi:10.18632/oncotarget.14528.
24. Alsarraj J, et al. BRD4 short isoform interacts with RRP1B, SIPA1 and components of the LINC complex at the inner face of the nuclear membrane. PloS one. 2013;8:e80746. doi:10.1371/journal.pone.0080746.
25. Oh TI, Lee YM, Lim BO, Lim JH. Inhibition of NAT10 Suppresses Melanogenesis and Melanoma Growth by Attenuating Microphthalmia-Associated Transcription Factor (MITF) Expression. Int J Mol Sci 18, doi:10.3390/ijms18091924 (2017).
26. Han F, Liu HQ, Wang SY. [Expression of CD117, MITF and NAT10 and their prognostic values in sinonasal mucosal melanoma]. Zhonghua bing li xue za zhi = Chinese journal of pathology. 2018;47:931–5. doi:10.3760/cma.j.issn.0529-5807.2018.12.007.
27. Martin RD, Hébert TE, Tanny JC. Therapeutic Targeting of the General RNA Polymerase II Transcription Machinery. Int J Mol Sci 21, doi:10.3390/ijms21093354 (2020).
28. Rimel JK, et al. Selective inhibition of CDK7 reveals high-confidence targets and new models for TFIIH function in transcription. Genes Dev. 2020;34:1452–73. doi:10.1101/gad.341545.120.
29. Peissert S, Schlosser A, Kendel R, Kuper J, Kisker C. Structural basis for CDK7 activation by MAT1 and Cyclin H. Proc Natl Acad Sci USA. 2020;117:26739–48. doi:10.1073/pnas.2010885117.
30. Sava GP, Fan H, Coombes RC, Buluwela L, Ali S. CDK7 inhibitors as anticancer drugs. Cancer Metastasis Rev. 2020;39:805–23. doi:10.1007/s10555-020-09885-8.
31. Rossi DJ, et al. Inability to enter S phase and defective RNA polymerase II CTD phosphorylation in mice lacking Mat1. EMBO J. 2001;20:2844–56. doi:10.1093/emboj/20.11.2844.
32. Chou J, Quigley DA, Robinson TM, Feng FY, Ashworth A. Transcription-Associated Cyclin-Dependent Kinases as Targets and Biomarkers for Cancer Therapy. Cancer discovery. 2020;10:351–70. doi:10.1158/2159-8290.Cd-19-0528.
33. Zeng M, et al. Targeting MYC dependency in ovarian cancer through inhibition of CDK7 and CDK12/13. *eLife* **7**, doi:10.7554/eLife.39030 (2018).
34. Fisher RP. Cdk7: a kinase at the core of transcription and in the crosshairs of cancer drug discovery. Transcription. 2019;10:47–56. doi:10.1080/21541264.2018.1553483.
35. Wang Y, et al. CDK7-dependent transcriptional addiction in triple-negative breast cancer. Cell. 2015;163:174–86. doi:10.1016/j.cell.2015.08.063.

36. Zhang H, et al. CDK7 Inhibition Potentiates Genome Instability Triggering Anti-tumor Immunity in Small Cell Lung Cancer. Cancer cell. 2020;37:37–54.e39. doi:10.1016/j.ccell.2019.11.003.
37. Lu P, et al. THZ1 reveals CDK7-dependent transcriptional addictions in pancreatic cancer. Oncogene. 2019;38:3932–45. doi:10.1038/s41388-019-0701-1.
38. Zhang Y, et al. The Covalent CDK7 Inhibitor THZ1 Potently Induces Apoptosis in Multiple Myeloma Cells In Vitro and In Vivo. Clinical cancer research: an official journal of the American Association for Cancer Research. 2019;25:6195–205. doi:10.1158/1078-0432.Ccr-18-3788.
39. Wang R, Wang Y. Fourier Transform Infrared Spectroscopy in Oral Cancer Diagnosis. Int J Mol Sci 22, doi:10.3390/ijms22031206 (2021).
40. Mikkonen JJ, et al. Fourier Transform Infrared Spectroscopy and Photoacoustic Spectroscopy for Saliva Analysis. Appl Spectrosc. 2016;70:1502–10. doi:10.1177/0003702816654149.
41. Lindemann A, Takahashi H, Patel AA, Osman AA, Myers JN. Targeting the DNA Damage Response in OSCC with TP53 Mutations. Journal of dental research. 2018;97:635–44. doi:10.1177/0022034518759068.
42. Irfan M, Delgado RZR, Frias-Lopez J. The Oral Microbiome and Cancer. Frontiers in immunology. 2020;11:591088. doi:10.3389/fimmu.2020.591088.
43. Dong J, Thrift AP. Alcohol, smoking and risk of oesophago-gastric cancer. Best Pract Res Clin Gastroenterol. 2017;31:509–17. doi:10.1016/j.bpg.2017.09.002.
44. Ray S, et al. Exposure to chewing tobacco promotes primary oral squamous cell carcinoma and regional lymph node metastasis by alterations of SDF1α/CXCR4 axis. Int J Exp Pathol. 2021;102:80–92. doi:10.1111/iep.12386.
45. Abati S, Bramati C, Bondi S, Lissoni A, Trimarchi M. Oral Cancer and Precancer: A Narrative Review on the Relevance of Early Diagnosis. Int J Environ Res Public Health 17, doi:10.3390/ijerph17249160 (2020).
46. Ganesh D, et al. Potentially Malignant Oral Disorders and Cancer Transformation. Anticancer research. 2018;38:3223–9. doi:10.21873/anticanres.12587.
47. Matejcic M, Gunter MJ, Ferrari P. Alcohol metabolism and oesophageal cancer: a systematic review of the evidence. Carcinogenesis. 2017;38:859–72. doi:10.1093/carcin/bgx067.
48. Shimpi N, et al. Patient awareness/knowledge towards oral cancer: a cross-sectional survey. BMC oral health 18, 86, doi:10.1186/s12903-018-0539-x (2018).
49. Thomson PJ. Perspectives on oral squamous cell carcinoma prevention-proliferation, position, progression and prediction. Journal of oral pathology medicine: official publication of the International Association of Oral Pathologists the American Academy of Oral Pathology. 2018;47:803–7. doi:10.1111/jop.12733.
50. Bagan J, Sarrion G, Jimenez Y. Oral cancer: clinical features. Oral Oncol. 2010;46:414–7. doi:10.1016/j.oraloncology.2010.03.009.

51. Shin YJ, Choung HW, Lee JH, Rhyu IC, Kim HD. Association of Periodontitis with Oral Cancer: A Case-Control Study. Journal of dental research. 2019;98:526–33. doi:10.1177/0022034519827565.
52. Linsen SS, Gellrich NC, Krüskemper G. Age- and localization-dependent functional and psychosocial impairments and health related quality of life six months after OSCC therapy. Oral Oncol. 2018;81:61–8. doi:10.1016/j.oraloncology.2018.04.011.
53. Arnold M, Ferlay J, van Berge Henegouwen MI, Soerjomataram I. Global burden of oesophageal and gastric cancer by histology and subsite in 2018. Gut. 2020;69:1564–71. doi:10.1136/gutjnl-2020-321600.
54. Wagner S, et al. [HPV-associated head and neck cancer: mutational signature and genomic aberrations]. Hno. 2015;63:758–67. doi:10.1007/s00106-015-0074-x.
55. Wang Y, et al. Genetic variants in AKT1 gene were associated with risk and survival of OSCC in Chinese Han Population. Journal of oral pathology medicine: official publication of the International Association of Oral Pathologists the American Academy of Oral Pathology. 2015;44:45–50. doi:10.1111/jop.12211.
56. Zedan W, Mourad MI, El-Aziz SM, Salamaa NM, Shalaby AA. Cytogenetic significance of chromosome 17 aberrations and P53 gene mutations as prognostic markers in oral squamous cell carcinoma. Diagnostic pathology. 2015;10:2. doi:10.1186/s13000-015-0232-1.
57. Mazumder S, Datta S, Ray JG, Chaudhuri K, Chatterjee R. Liquid biopsy: miRNA as a potential biomarker in oral cancer. Cancer epidemiology. 2019;58:137–45. doi:10.1016/j.canep.2018.12.008.
58. Momen-Heravi F, Bala S. Emerging role of non-coding RNA in oral cancer. Cellular signalling. 2018;42:134–43. doi:10.1016/j.cellsig.2017.10.009.
59. Yao Y, et al. MiRNA-128 and MiRNA-142 Regulate Tumorigenesis and EMT in Oral Squamous Cell Carcinoma Through HOXA10. Cancer management research. 2020;12:9987–97. doi:10.2147/cmar.S250093.
60. He B, Lin X, Tian F, Yu W, Qiao B. MiR-133a-3p Inhibits Oral Squamous Cell Carcinoma (OSCC) Proliferation and Invasion by Suppressing COL1A1. Journal of cellular biochemistry. 2018;119:338–46. doi:10.1002/jcb.26182.
61. Li Q, et al. NAT10 is upregulated in hepatocellular carcinoma and enhances mutant p53 activity. BMC Cancer. 2017;17:605. doi:10.1186/s12885-017-3570-4.
62. Livak KJ, Schmittgen TD. Analysis of relative gene expression data using real-time quantitative PCR and the 2(-Delta Delta C(T)) Method. Methods. 2001;25:402–8. doi:10.1006/meth.2001.1262.

Figures

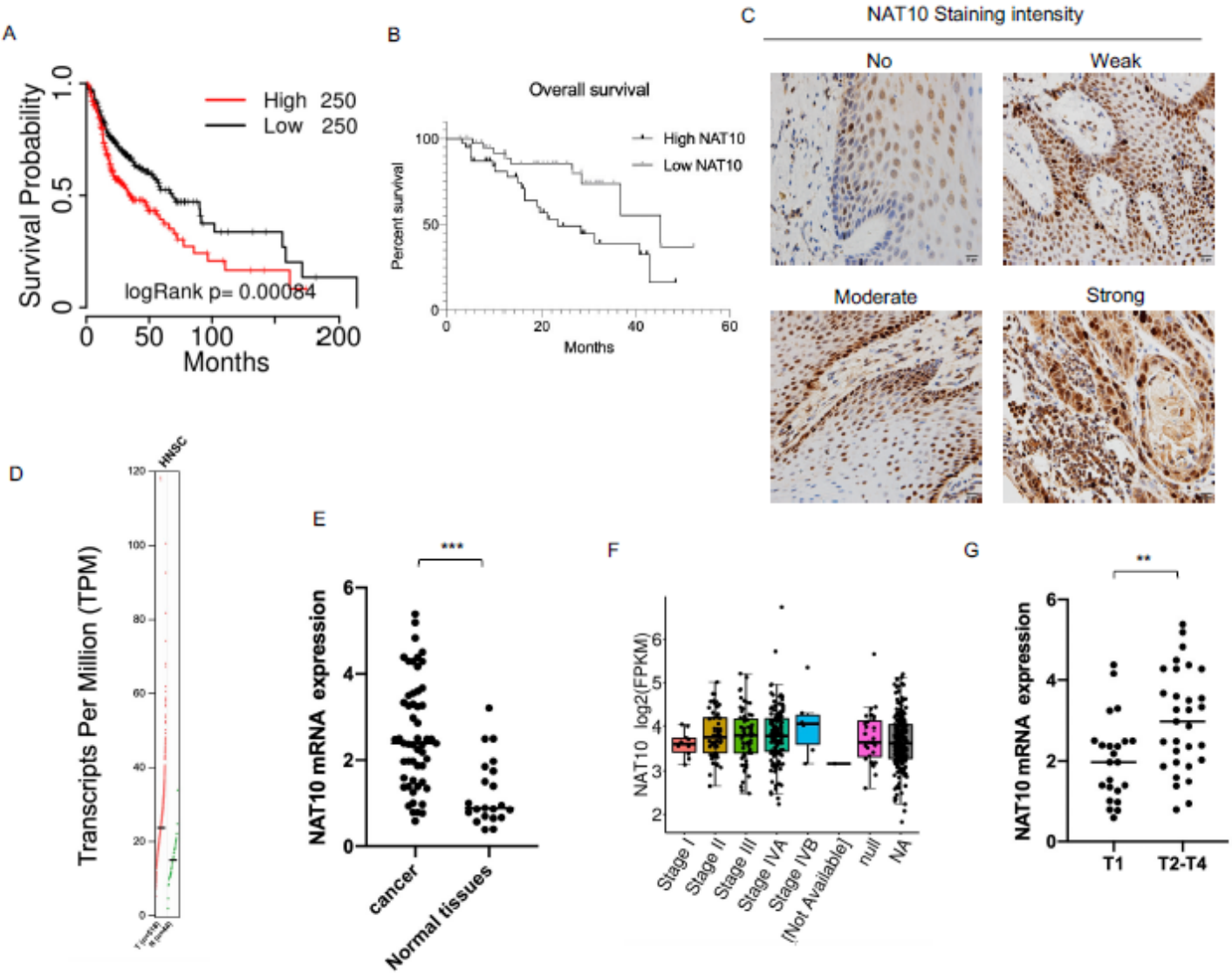

Figure 1

Identification of NAT10 Associated with Overall Survival (OS) in oral cancer (A) Kaplan-Meier curves of OS for 500 HNSCC patients from TCGA using TCGAportal online website with high or low NAT10 expression. (B) Kaplan-Meier curves of OS for 80 oral cancer patients with high or low NAT10 expression. (C) Representative IHC images of NAT10 expression are shown. Scale bars,20μm. (D) Cholangiocarcinoma tissues and adjacent normal tissues were subjected to mRNA analysis using TCGAportal online website. (E) 54 cases cholangiocarcinoma tissues and 21 cases adjacent normal tissues were subjected to mRNA analysis using RT-PCR. (G) TCGAportal website was used to analyze the mRNA level of oral cancer patients at different stages. (G) RT-PCR was used to analyze the mRNA level of oral cancer patients at T1 and T2-T4 stage.

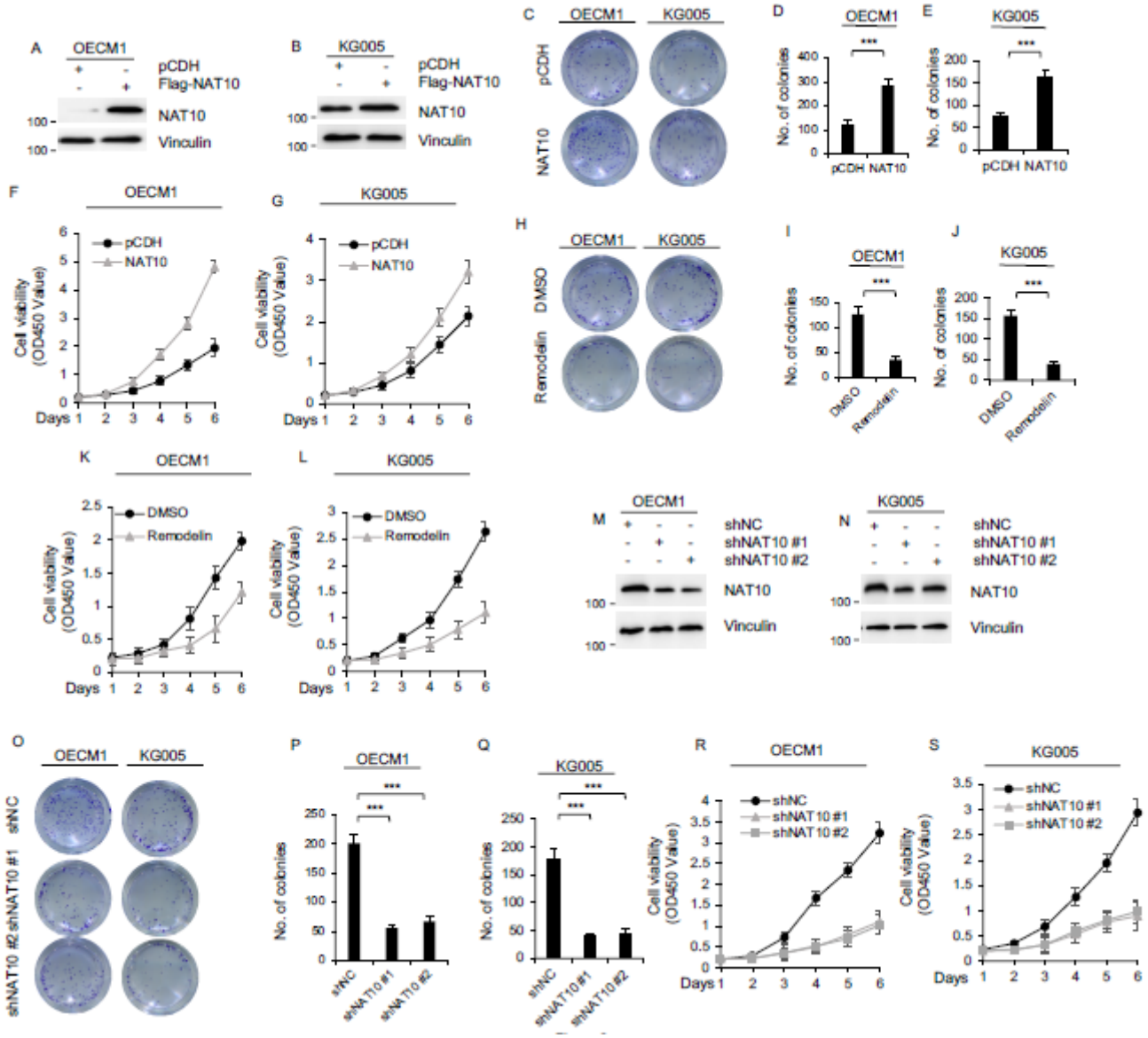

Figure 2

NAT10 promotes oral cancer proliferation in vitro (A-B) OECM1 (A) and KG005 (B) cells stably expresseing pCDH and Flag-NAT10 were analyzed by immunoblotting. (C-G) OECM1 and KG005 cells stably expressing pCDH and Flag-NAT10 were subjected to cell proliferation assays by colony growth (C-E) and CCK-8 assays (F-G). (H-L) OECM1 and KG005 cells added with DMSO or remodelin were subjected to cell proliferation assays by colony growth (H-J) and CCK-8 assays (K-L). (M-N) OECM1 (M) and KG005 (N) cells stably expresseing shNC, shNAT10#1 and shNAT10#2 were analyzed by immunoblotting. (O-S) OECM1 and KG005 cells stably expresseing shNC, shNAT10#1 and shNAT10#2 were subjected to cell proliferation assays by colony growth (O-Q) and CCK-8 assays (R-S).

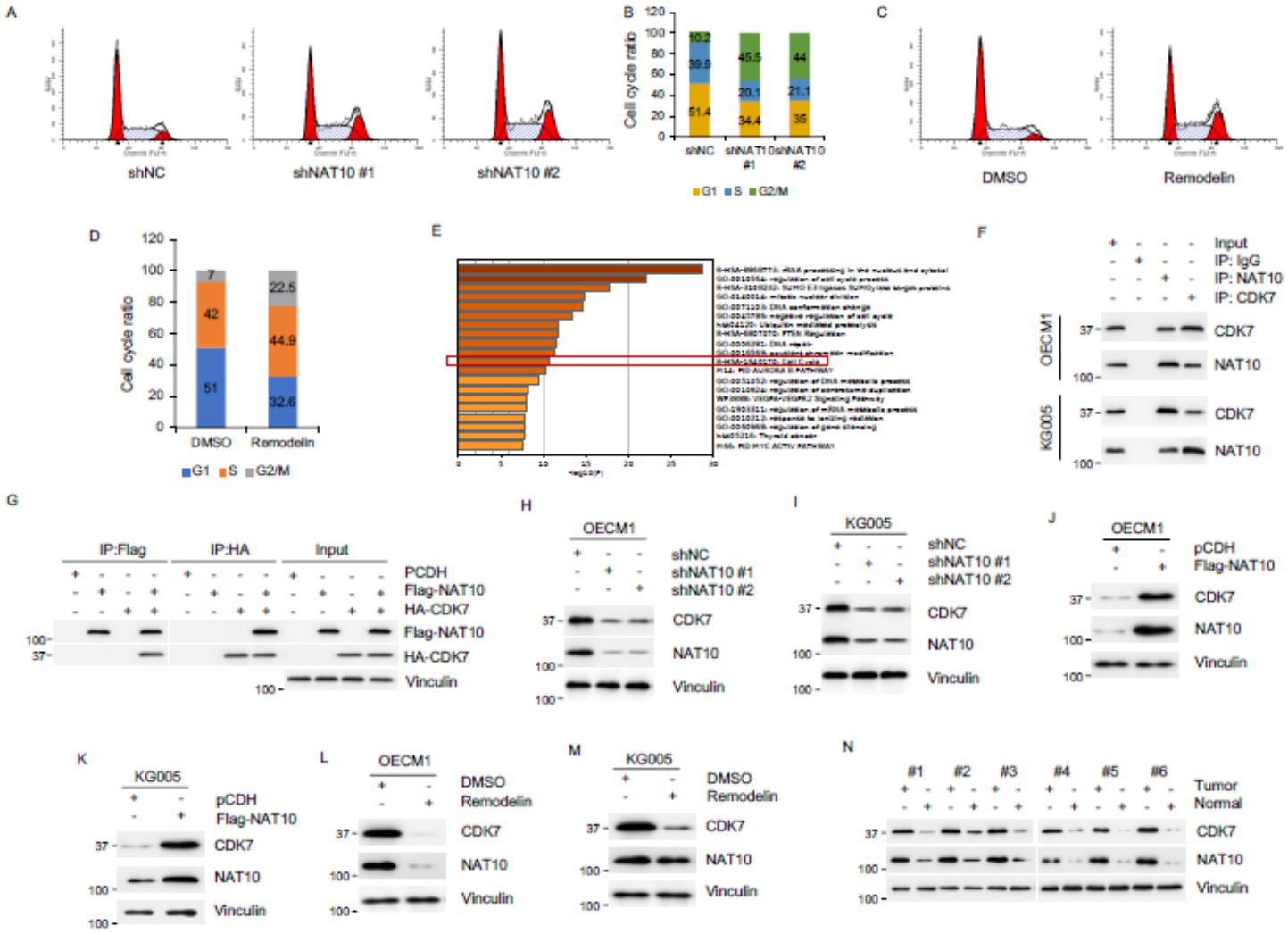

Figure 3

NAT10 interacts with CDK7 and regulates its expressing level (A-B) OECM1 cells stably expresseing shNC, shNAT10#1 and shNAT10#2 were performed with flow cytometry to analyze cell cycle. (C-D) OECM1 cells added with DMSO and remodelin were performed with flow cytometry to analyze cell cycle. (E) GO analysis was performed in the proteins interacted with NAT10. (F) Lysates from OECM1 and KG005 cells were immunoprecipitated with control IgG, an anti- NAT10 or an anti-CDK7 antibody, followed by immunoblotting analysis. (G) Lysates from HEK293T cells transiently expressed Flag-NAT10 and HA-CDK7 were immunoprecipitated with anti-Flag or an anti-HA antibody, followed by immunoblotting analysis. (H-I) OECM1 and KG005 cells stably expressing shNC, shNAT10 #1 and shNAT10 #2 were analyzed by immunoblotting using indicated antibody. (J-K) OECM1 and KG005 cells stably expressing pCDH and Flag-NAT10 were analyzed by immunoblotting using indicated antibody. (L-M) OECM1 and KG005 cells added with DMSO and remodelin were analyzed by immunoblotting using indicated antibody. (N) Six pairs of cholangiocarcinoma tissues and adjacent normal tissues were analyzed by immunoblotting using indicated antibody.

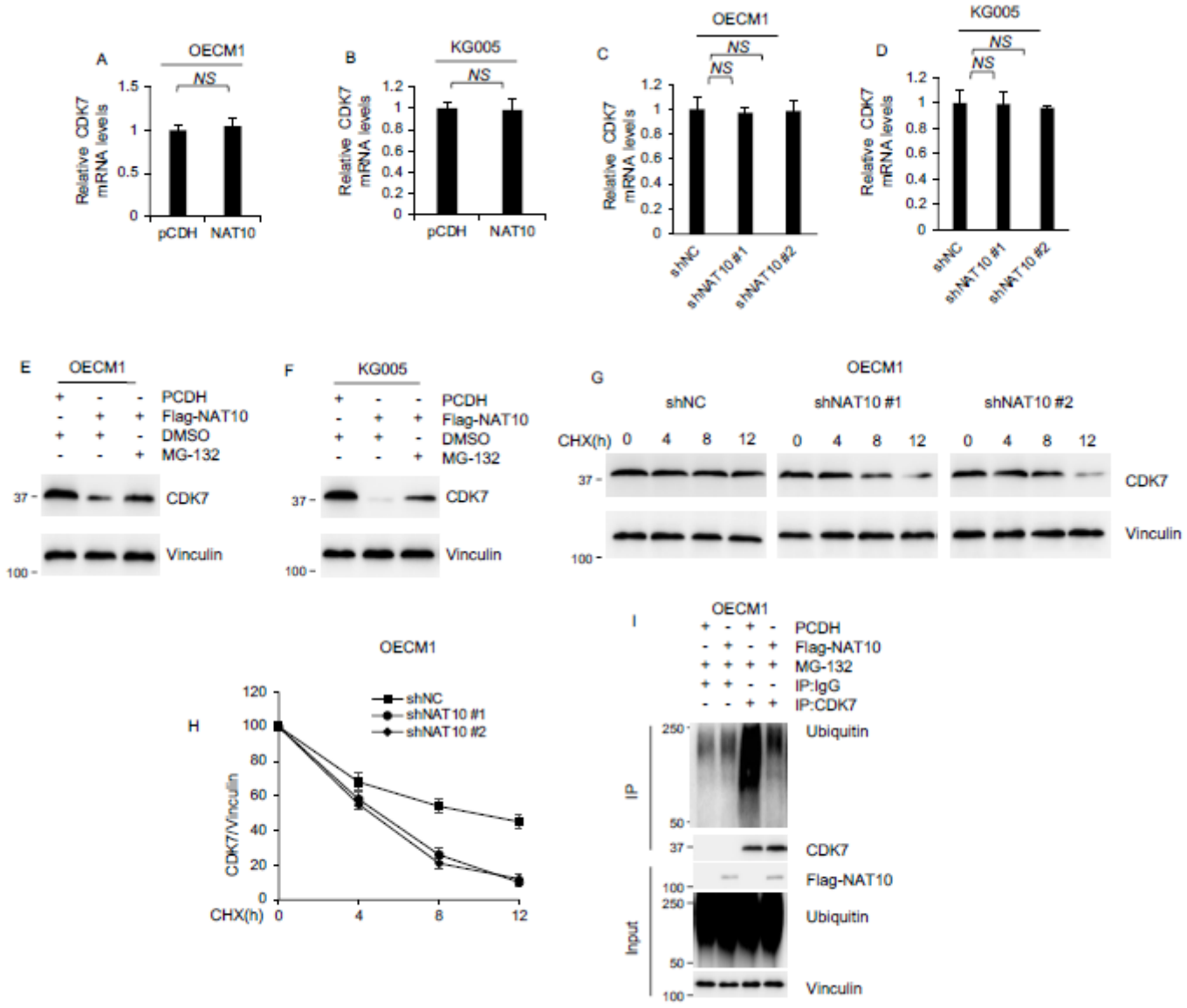

Figure 4

NAT10 regulates CDK7 at level of protein post translational modification (A-B) OECM1 and KG005 cells stably expresseing pCDH and NAT10 were performed mRNA analysis using RT-PCR. (C-D) OECM1 and KG005 cells stably expresseing shNC, shNAT10 #1 and shNAT10 #2 were performed mRNA analysis using RT-PCR. (E-F) OECM1 and KG005 cells stably expresseing pCDH and NAT10 were treated with DMSO or 20 μM MG-132 for 6 h, then subjected to immunoblotting analysis with the indicated antibodies. (G-H) 100 μg/mL of CHX was used to treat OECM1 Cells which stably expressed both shNC, shNAT10 #1 and shNAT10 #2 for the indicated times, which were analyzed by immunoblotting. (I) OECM1 cells stably expresseing pCDH and NAT10 were performed immunoprecipitation, then subjected to immunoblotting analysis with the indicated antibodies. OECM1 cells were treated with 20 μM MG-132 for 6 h before harvest.

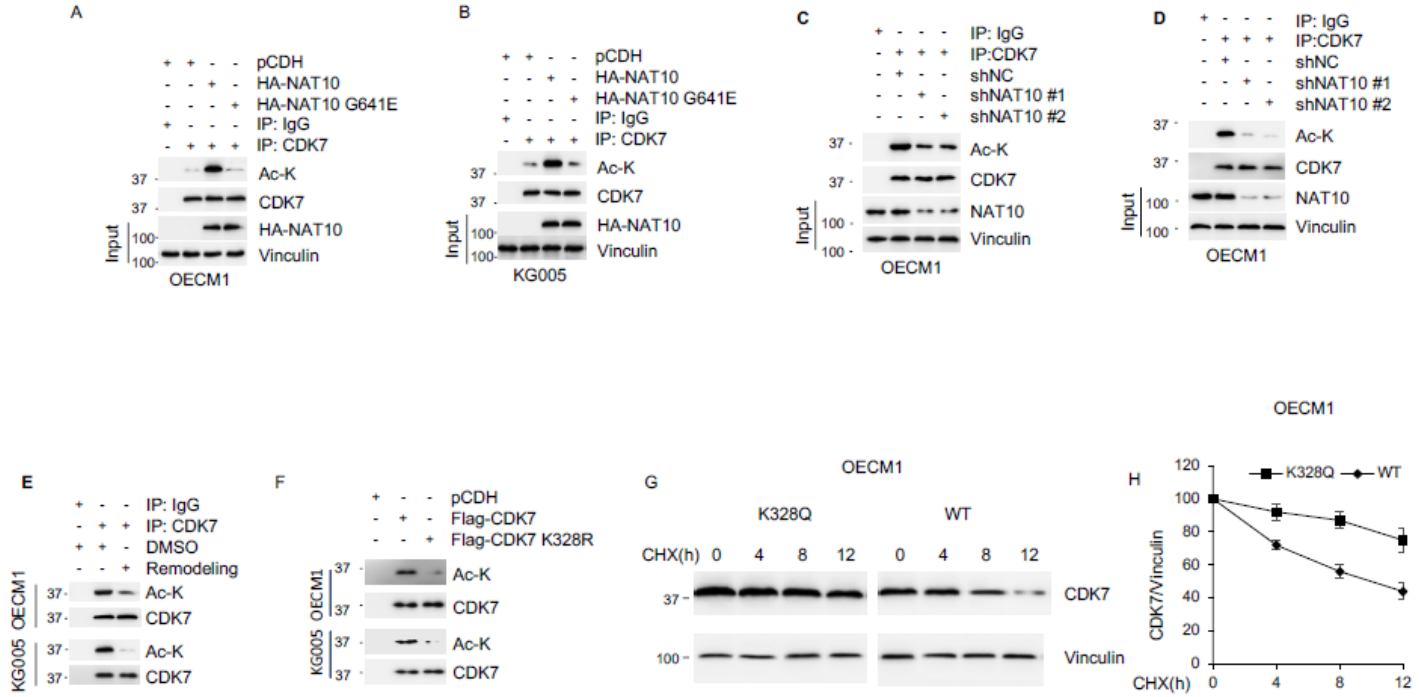

Figure 5

NAT10 promotes the acetylation of CDK7 (A-B) OECM1 and KG005 cells stably expressing pCDH, NAT10 and NAT10 G641 were subjected to immunoprecipitation, then analyzed by immunoblotting using indicated antibody. (C-D) OECM1 and KG005 cells stably expressing shNC and shNAT10 #1 and shNAT10 #2 were subjected to immunoprecipitation, then analyzed by immunoblotting using indicated antibody. (E) OECM1 cells treated with DMSO or remodelin were subjected to immunoprecipitation, then analyzed by immunoblotting using indicated antibody. (F) OECM1 cells stably expressing pCDH, CDK7 and NAT10 K328R were subjected to immunoprecipitation, then analyzed by immunoblotting using indicated antibody. (G-H) 100 μg/mL of CHX was used to treat OECM1 Cells which stably expressed both CDK7 K328Q and CDK7 for the indicated times, which were analyzed by immunoblotting.

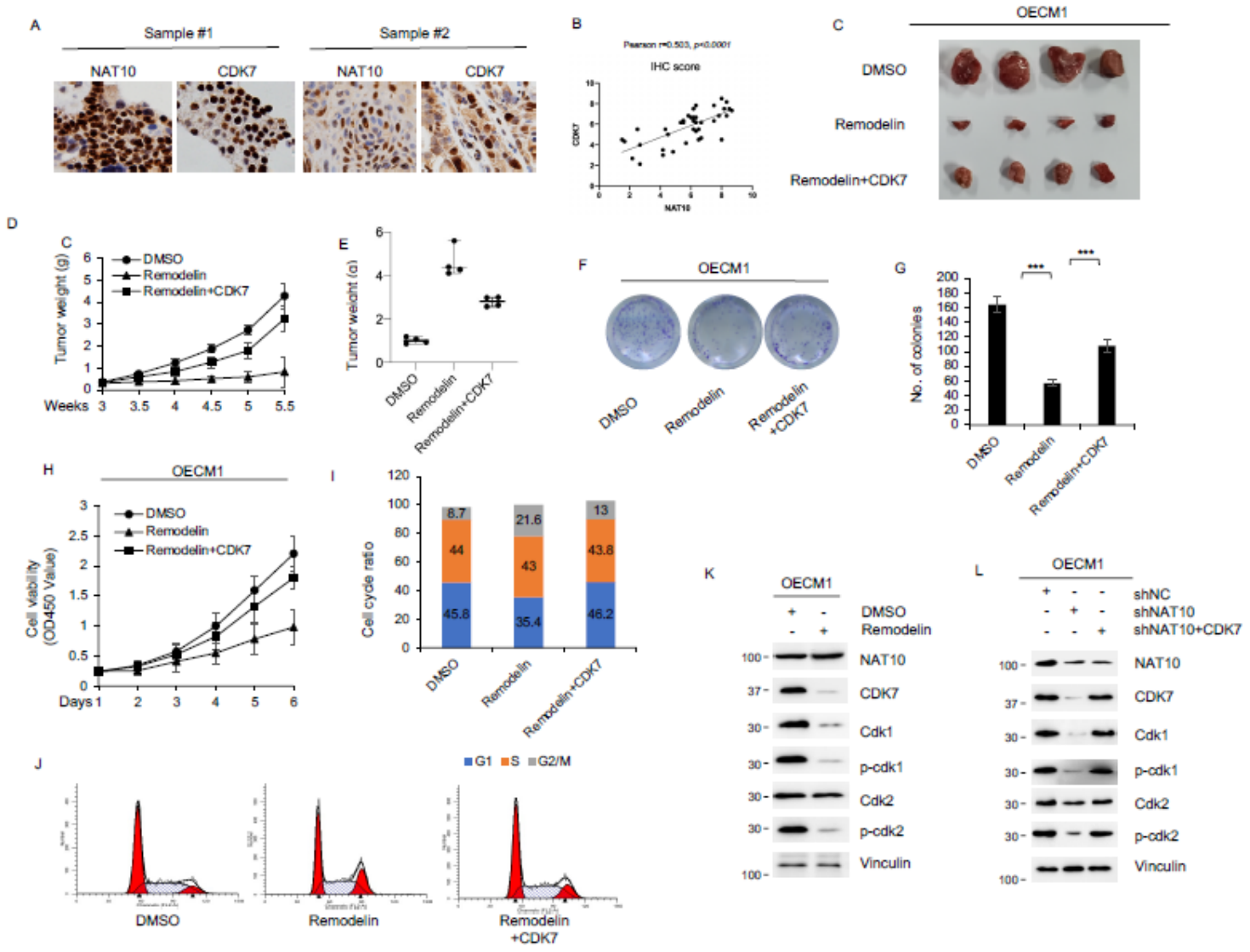

Figure 6

NAT10 promoted growth of oral cancer through CDK7 (A-B) 54 clinical samples were subjected to IHC analysis with the indicated antibodies. Representative images are shown. Scale bars, 20 μm. (C-E) OECM1 cells treated with DMSO or remodelin and stably re-expressing CDK7 in combination were injected into flank region of 6-week-old male athymic Balb/c nude mice (n=4). After 5.5 weeks of injected, xenograft tumors were harvested. Tumor growth curves (D), photographs of harvested tumors (C), and tumor weight (E) are shown. (F-H) OECM1 cells treated with DMSO or remodelin and stably re-expressing CDK7 in combination were subjected to cell proliferation assays by colony growth assays. (I-J) OECM1 treated with DMSO or remodelin and stably re-expressing CDK7 in combination were performed with flow cytometry to analyze cell cycle. (K) OECM1 treated with DMSO or remodelin were analyzed by immunoblotting using indicated antibody. (L) OECM1 shNC, shNAT10 and re-expressing CDK7 alone or in combination were analyzed by immunoblotting using indicated antibody.

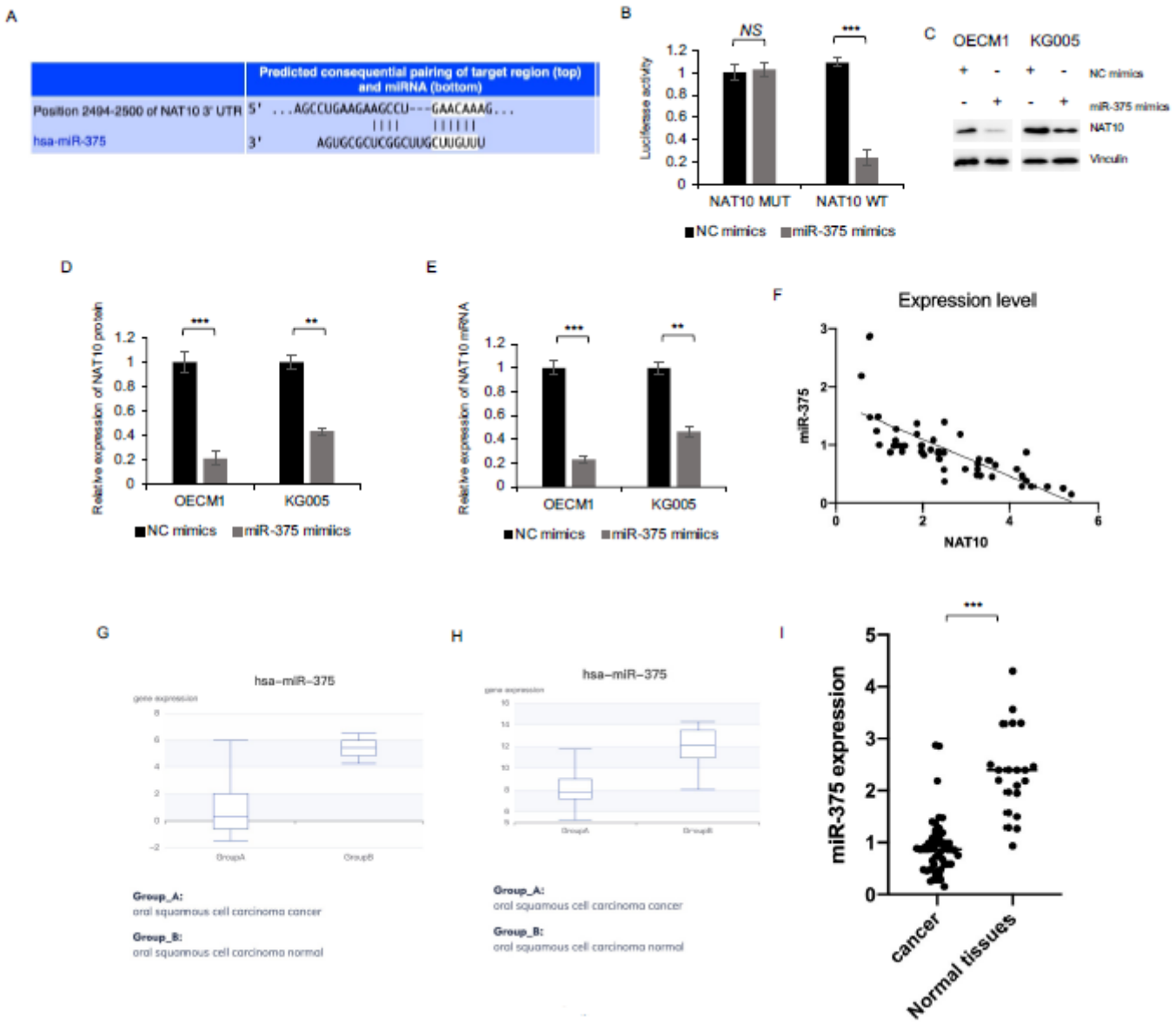

Figure 7

NAT10 serve as a target of miR-375 (A) Predicted binding site between miR-375 and the 3'UTR of NAT10. (B) The binding relationship between miR-375 and NAT10 3'UTR was verified by dual luciferase reporter gene assay. (C-D) Immunoblotting was used to detect the expression protein levels of NAT10 in NC mimics and miR-375 mimics OECM1 and KG005 cells. (E) qRT-PCR was used to detect the expression mRNA levels of NAT10 in NC mimics and miR-375 mimics OECM1 and KG005 cells. (F) 54 clinical samples were subjected to expression analysis with the indicated antibodies. Representative images are shown. Scale bars, 20 μm. (G-H) The expression of miR-375 was predicted using online website. (I) 54 cases cholangiocarcinoma tissues and 21 cases adjacent normal tissues were subjected to mRNA analysis using RT-PCR.

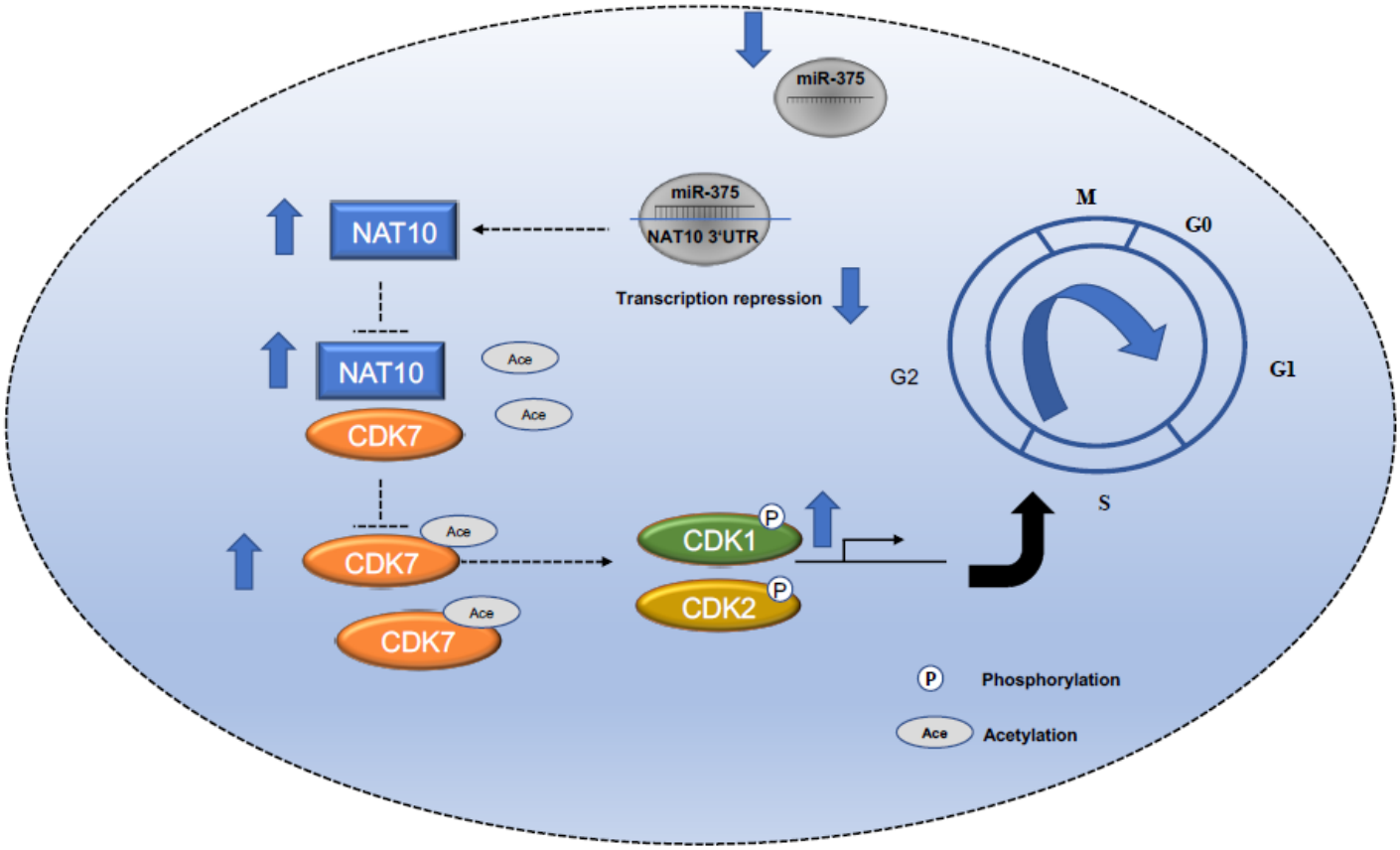

Figure 8

NAT10-CDK7 axis plays a facilitative role in oral cancer progression NAT10 elicited tumor facilitative role by ubiquitinating CDK7. Knockdown of CDK7 decimated NAT10-mediated promotion of proliferation. NAT10 positively regulated the phosphorylation level of CDK1 and CDK2 through CDK7 thus involved in cell cycle of cholangiocarcinoma. Furthermore, NAT10 is regulated by upstream miR-375. Compared adjacent normal tissue, miR-375 is downregulated in oral cancer, thus inhibited transcription of NAT10. In conclusion, NAT10-CDK7 axis plays a contributory role in oral cancer and serves as a biomarker for the treatment and diagnosis of oral cancer.

Supplementary Files

This is a list of supplementary files associated with this preprint. Click to download.

- supplementaryfigures.pdf